

Electrical Conductivity and Luminescence in Coordination Polymers Based on Copper(I)-Halides and Sulfur-Pyrimidine Ligands

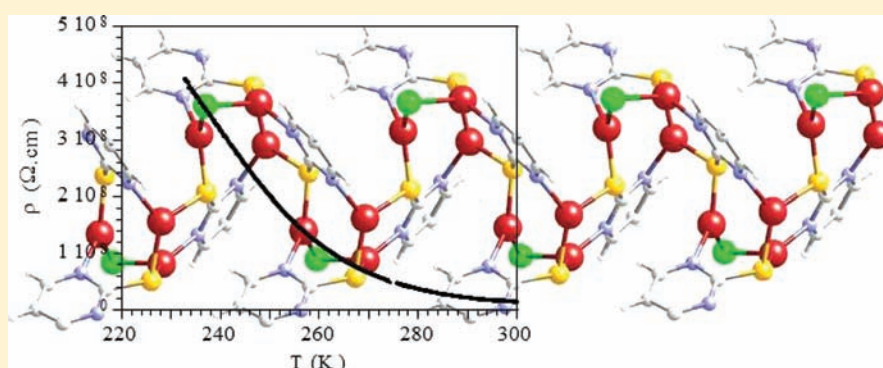
Almudena Gallego,[†] Oscar Castillo,[‡] Carlos J. Gómez-García,[§] Félix Zamora,^{*,†} and Salome Delgado^{*,†}

[†]Departamento de Química Inorgánica, Universidad Autónoma de Madrid, 28049 Madrid, Spain

[‡]Departamento de Química Inorgánica, Facultad de Ciencia y Tecnología, Universidad del País Vasco, Apartado 644, E-48080 Bilbao, Spain

[§]Instituto de Ciencia Molecular, Parque Científico de la Universidad de Valencia, 46980 Paterna, Valencia, Spain

S Supporting Information



ABSTRACT: The solvothermal reactions between pyrimidinedisulfide (pym_2S_2) and CuI or CuBr_2 in $\text{CH}_2\text{Cl}_2:\text{CH}_3\text{CN}$ lead to the formation of $[\text{Cu}_{11}\text{I}_7(\text{pymS})_4]_n$ (pymSH = pyrimidine-2(1*H*)-thione) (1) and the dimer $[\text{Cu}^{\text{II}}(\mu\text{-Br})(\text{Br})\text{L}]_2$ (L = 2-(pyrimidin-2-ylamino)-1,3-thiazole-4-carbaldehyde) (2). In the later reaction, there is an in situ S–S, S–C(sp^2), and C(sp^2)–N multiple bond cleavage of the pyrimidinedisulfide resulting in the formation of 2-(pyrimidin-2-ylamino)-1,3-thiazole-4-carbaldehyde. Interestingly, similar reactions carried out just with a change in the solvent ($\text{H}_2\text{O}:\text{CH}_3\text{CN}$ instead of $\text{CH}_2\text{Cl}_2:\text{CH}_3\text{CN}$) give rise to the formation of coordination polymers with rather different architectures. Thus, the reaction between pym_2S_2 and CuI leads to the formation of $[\text{Cu}_3\text{I}(\text{pymS})_2]_n$ (3) and $[\text{CuI}(\text{pym}_2\text{S}_3)]$ (pym_2S_3 = pyrimidiltrisulfide) (4), while $[\text{Cu}_3\text{Br}(\text{pymS})_2]_n$ (5) is isolated in the reaction with CuBr_2 . Finally, the solvothermal reactions between CuI and pyrimidine-2-thione (pymSH) in $\text{CH}_2\text{Cl}_2:\text{CH}_3\text{CN}$ at different ratios, 1:1 or 2:1, give the polymers $[\text{Cu}_2\text{I}_2(\text{pymSH})_2]_n$ (6) and $[\text{Cu}_2\text{I}_2(\text{pymSH})]_n$ (7), respectively. The structure of the new compounds has been determined by X-ray diffraction. The studies of the physical properties of the novel coordination polymers reveal that compounds 3 and 5 present excellent electrical conductivity values at room temperature, while compounds 1, 3, and 5–7 show luminescent strong red emission at room temperature.

INTRODUCTION

Coordination polymers have gained major attention in recent years in the field of materials science¹ due to their interesting properties including magnetism,² catalysis,³ nonlinear optics,⁴ molecular wires,^{5–8} and molecular sensing.^{9,10} A wide range of one-, two-, and three-dimensional architectures of coordination polymers have already been reported, but there are still many structures not yet prepared that may produce a variety of novel materials.

Hydro(solvo)thermal methods have proven to be a fruitful strategy in the preparation of highly stable coordination polymers with novel structural possibilities. This is in part due to the in situ metal/ligand reactions that can take place during the preparation process,¹¹ including redox, ligand oxidative coupling, and substitution reactions, and open alternative routes toward the discovery of new organic

reactions, the elucidation of reaction mechanisms, and the generation of novel functional materials, particularly for those that are inaccessible, or not easily attainable, by means of other conventional synthesis.¹²

On the other hand, organodisulfides exhibit a broad number of binding modes in their coordination abilities to metal ions.^{13–19} Indeed, they show rich redox chemistry based on both oxidative formation and reductive cleavage of the disulfide bonds. Additionally, the in situ cleavage of S–S or both S–S and S–C(sp^2) bonds in dithiodipyridine ligands has been recently reported under solvothermal conditions in the presence of certain metal ions (Co^{2+} or Cu^{2+}), enhancing its versatility under solvothermal conditions.^{20–23} Likewise, we

Received: October 18, 2011

Published: December 7, 2011

Table 1. Single-Crystal Data and Structure Refinement Details

	2	4	5	6	7
formula	C ₈ H ₆ Br ₂ CuN ₄ OS	C ₈ H ₆ CuIN ₄ S ₃	C ₈ H ₆ BrCu ₃ N ₄ S ₂	C ₈ H ₈ Cu ₂ I ₂ N ₄ S ₂	C ₄ H ₄ Cu ₂ I ₂ N ₂ S
<i>M_r</i>	429.59	444.79	492.82	605.18	493.03
crystal system	monoclinic	orthorhombic	monoclinic	triclinic	triclinic
space group	<i>P</i> 2 ₁ / <i>c</i> (no. 14)	<i>Pnma</i> (no. 62)	<i>P</i> 2 ₁ / <i>c</i> (no. 14)	<i>P</i> $\bar{1}$ (no. 2)	<i>P</i> $\bar{1}$ (no. 2)
<i>a</i> (Å)	10.0317(3)	7.4545(7)	10.3368(3)	7.2574(6)	7.3069(4)
<i>b</i> (Å)	9.8261(3)	15.4787(15)	7.6318(3)	7.9897(7)	8.0037(4)
<i>c</i> (Å)	12.7639(4)	11.1325(10)	17.4468(6)	13.9518(10)	8.5871(4)
α (°)				74.600(3)	97.410(2)
β (°)	114.520(2)		120.782(2)	81.066(3)	100.887(2)
γ (°)				63.818(3)	111.137(2)
<i>V</i> (Å ³)	1144.70(6)	1284.5(2)	1182.45(7)	699.24(10)	449.20(4)
<i>Z</i>	4	4	4	2	2
<i>D</i> _{calcd} (Mg/m ³)	2.493	2.300	2.768	2.874	3.645
crystal size (mm ³)	0.12 × 0.10 × 0.06	0.20 × 0.20 × 0.15	0.09 × 0.07 × 0.02	0.25 × 0.20 × 0.10	0.25 × 0.25 × 0.10
color	brown	orange	orange	red	red
<i>F</i> (000)	820	848	944	560	444
μ (mm ⁻¹)	12.495	25.689	9.059	7.740	11.772
<i>R</i> _{int}	0.0356	0.0348	0.0346	0.0392	0.0565
reflns collected	8950	9661	4817	12560	14360
reflns independent	2161	1270	2343	3052	1785
reflns unique [<i>I</i> > 2 σ (<i>I</i>)]	1914	1255	1708	2897	1754
parameters	154	82	163	163	100
GOF (<i>S</i>) ^a	1.094	1.113	0.908	1.129	1.181
<i>R</i> ₁ / <i>wR</i> ₂ [<i>I</i> ≥ 2 σ (<i>I</i>)] ^b	0.0463/0.1347	0.0244/0.0621	0.0311/0.0679	0.0268/0.0702	0.0272/0.0636
<i>R</i> ₁ / <i>wR</i> ₂ (all data) ^c	0.0527/0.1421	0.0246/0.0624	0.0472/0.0696	0.0286/0.0735	0.0278/0.0639

^a*S* = $[\sum w(|F_o| - |F_c|)^2 / (N_{\text{obsd}} - N_{\text{param}})]^{1/2}$. ^b*R*₁ = $\Sigma(|F_o| - |F_c|) / \Sigma |F_o|$; *wR*₂ = $[\sum w(F_o^2 - F_c^2)^2 / \sum w F_o^2]^{1/2}$. ^c*w* = $1/[\sigma^2(F_o^2) + (AP)^2]$; *P* = $(F_o^2 + 2F_c^2)/3$.

have reported for the first time the S–S, S–C(sp²), and N–C(sp²) multicleavage bonds in the solvothermal and solvothermal microwave reactions of bis(2-pyrimidyl)disulfide with CuCl₂.²⁴

Additionally, the use of heterocyclic thiones has attracted interest due to the fact that they can behave either as ambidentate or multifunctional donor ligands, binding to metal centers via exocyclic sulfur or heterocyclic nitrogen atoms. Thus, pyrimidine-2(1*H*)-thione (pymSH) and its corresponding thiolate form (pymS[−]) may adopt different coordination modes. This versatility enables the formation of a large variety of coordination complexes, including coordination polymers with novel and interesting structures. However, little structural studies have been reported so far on the coordination polymers with pymSH. This is probably due to the difficulties to obtain suitable single crystals for their structural determination by X-ray diffraction.

In this sense, it is well-established that the pymSH/pymS[−] and bis(2-pyrimidyl)disulfide (pym₂S₂) ligands are good coordinating ligands toward soft Lewis acids such as Cu(I). However, the reaction rates between Cu(I) and pymSH/pymS[−] are so fast that typically uncharacterized precipitates are immediately formed.^{15–19,25–28} A novel strategy to solve this problem consists in using very diluted solutions of reactants to allow slow diffusion conditions.²⁹ Following this procedure, halides readily coordinate to copper(I), due to the soft–soft bonding preference, and the polymers [Cu(pymSH)*X*]_{*n*} (*X* = Cl and Br) are isolated as single crystals from very dilute solutions.²⁹

Finally, it is worth mentioning that it appears that metal–sulfur–organic networks constitute a class of promising electronic materials due to their electronic properties (e.g.,

electrical conductivity).^{30,31} The incorporation of thiolate-S acting as a bridging ligand between adjacent transition metal centers in coordination polymers is highly desirable in terms of magnetic, electrical conductivity, and optical properties. This is due to the fact that the metal orbital energies are better matched for sulfur, leading to a higher delocalization of spin density through the bridging atoms.³² In fact, we have been recently able to obtain a highly semiconducting 1D coordination polymer based on Cu(I) and 2,2'-dipyridyldisulfide.³³ Additionally, compounds based on Cu(I) and halides have shown interesting luminescence properties, even at room temperature, showing that emission highly depends on the structure and metal environment, which is related to closed-shell copper(I)/copper(I) interactions.³⁴

Following our research on the preparation of copper coordination polymers with organosulfur ligands,^{35–37} in this work, we have focused on the synthesis of novel luminescent and conducting materials based on coordination polymers. As we have previously established that copper coordination polymers containing organosulfur ligands are suitable candidates to reach this goal,^{32,33} in this manuscript, we report a study of the reactions between the pyrimidine-2(1*H*)-thione (pymSH) and bis(2-pyrimidyl)disulfide (pym₂S₂) ligands with CuI and CuBr₂ under solvothermal conditions. This study has led to the synthesis of up to seven different compounds depending on the solvent, ligand, and precursor copper salt. Thus, the reaction of bis(2-pyrimidyl)disulfide (pym₂S₂) and CuI or CuBr₂ in CH₂Cl₂:CH₃CN gives [Cu₁₁I₇(pymS)₄]_{*n*} (1) and the dimer [Cu^{II}(μ-Br)(Br)L]₂ [L = 2-(pyrimidin-2-ylamino)-1,3-thiazole-4-carbaldehyde] (2). A change of the solvent in the previous reactions (H₂O:CH₃CN instead of CH₂Cl₂:CH₃CN) yielded [Cu₃I(pymS)₂]_{*n*} (3) and [CuI-

(pym_2S_3)] (**4**) (with CuI) and $[\text{Cu}_3\text{Br}(\text{pymS})_2]_n$ (**5**) (with CuBr_2). Finally, reaction of CuI with a different ligand, pyrimidine-2(1*H*)-thione (pymSH), in $\text{CH}_2\text{Cl}_2:\text{CH}_3\text{CN}$ with different ratios (1:1 or 2:1) lead to the polymers $[\text{Cu}_2\text{I}_2(\text{pymSH})_2]_n$ (**6**) and $[\text{Cu}_2\text{I}_2(\text{pymSH})]_n$ (**7**).

EXPERIMENTAL SECTION

Materials and Methods. All chemicals were of reagent grade and were used as commercially obtained. The pyrimidinedisulfide (pym_2S_2) ligand was prepared according to the published procedure.³⁸ FTIR spectra (KBr pellets) were recorded on a Perkin-Elmer 1650 spectrophotometer. Elemental analyses were performed by the Microanalysis Service of the Universidad Autónoma de Madrid on a Perkin-Elmer 240 B microanalyzer.

DC electrical conductivity measurements were carried out on several crystals for each compound. We perform two different measurements: (i) With two contacts at 300 K, the contacts between the crystals and the platinum wires (0.3 mm, 65 diameter) were made using two tungsten tips. The samples were measured by applying an electrical current of voltages from +10 to -10 V. (ii) With four contacts at variable temperature, the contacts were made with Pt wires (25 μm diameter) along the long axis of the needles using graphite paste. The samples were measured in a Quantum Design PPMS-9 with DC currents in the range 10–100 nA. The cooling and warming rate was 0.2–0.5 K/min, and the results were, within experimental error, similar in both scans and intensity independent.

Luminescence excitation and emission spectra of the solid compounds were performed at 25 °C on a 48000s (T-Optics) spectrofluorometer from SLM-Aminco. A front face sample holder was used for data collection and oriented at 60° to minimize light scattering from the excitation beam on the cooled R-928 photomultiplier tube. Appropriate filters were used to eliminate Rayleigh and Raman scatters from the emission. Excitation and emission spectra were corrected for the wavelength dependence of the 450 W xenon arc excitation but not for the wavelength dependence of the detection system. Spectroscopic properties were measured by reflection (front face mode) on finely ground samples and placed in quartz cells of 1 mm path length. No attempt was made to remove adsorbed or dissolved molecular oxygen from the materials. Reference samples that do not contain any fluorescent dopant were used to check the background and optical properties of the samples.

X-ray Data Collection and Crystal Structure Determination.

Crystal data were collected, at 100 K, on a Bruker SMART 6K CCD diffractometer (Cu $K\alpha$ radiation, $\lambda = 1.54178 \text{ \AA}$) (compounds **2** and **4**) and on an Oxford Diffraction Xcalibur diffractometer (Mo $K\alpha$ radiation, $\lambda = 0.71073 \text{ \AA}$) (compounds **5**–**7**). The structures were solved by standard Patterson methods and refined by full-matrix least-squares methods based on F^2 using the SHELXL-97³⁹ and WinGX⁴⁰ programs. All nonhydrogen atoms were refined anisotropically, and the hydrogen atoms were included in geometrically calculated positions and refined isotropically according to the riding model. Crystal data, data collection, and refinement parameters for compounds **2** and **4**–**7** are summarized in Table 1.

Synthesis and Characterization. *Solvothermal Synthesis of $[\text{Cu}_{117}(\text{pymS})_4]_n$ (**1**).* A mixture of CuI (134 mg, 0.7 mmol) and bis(2-pyrimidyl)disulfide (pym_2S_2) (156 mg, 0.7 mmol) was stirred for 30 min in 26 mL of a $\text{CH}_2\text{Cl}_2:\text{CH}_3\text{CN}$ mixture (1:1 in volume) and sealed in a 45 mL Teflon-lined autoclave. The reactor was heated at 90 °C for 20 h and then slowly cooled down to room temperature at a rate of 2.5 °C per hour. Red block crystals of **1** were obtained, washed with ether, and dried on air (67 mg, 52% yield based on Cu). Anal. calcd (%) for $\text{C}_{16}\text{H}_{12}\text{Cu}_{11}\text{I}_7\text{N}_8\text{S}_4$: C, 9.46; H, 0.60; N, 5.51; S, 6.31. Found (%): C, 9.38; H, 0.82; N, 5.47; S, 6.23. IR (KBr, cm^{-1}): 1553 (s), 1374 (vs), 1168 (s), 820 (m), 805 (m), 756 (m), 744 (m). When the mother solution (once the crystals of **1** were isolated) was left at room temperature for 1 week, yellow crystals of $[\text{Cu}_2(\text{pym}_2\text{S}_2)\text{I}_2]_2$ were isolated²⁵ (12 mg, yield 5% based on Cu).

*Solvothermal Synthesis of $[\text{Cu}^{\text{II}}(\mu\text{-Br})(\text{Br})\text{L}_2]_2$ (**2**) [$\text{L} = 2\text{-Pyrimidin-2-ylamino-1,3-thiazole-4-carbaldehyde}$].* A mixture of CuBr_2 (157

mg, 0.7 mmol) and pym_2S_2 (156 mg, 0.7 mmol) was stirred for 30 min in 26 mL of a $\text{CH}_2\text{Cl}_2:\text{CH}_3\text{CN}$ mixture (1:1 in volume) and sealed in a 45 mL Teflon-lined under analogous conditions. The solution obtained was allowed to stand at 0 °C for 2 weeks. The brown crystals formed (compound **2**) were filtered, washed with Et_2O , and dried in air (83 mg, 55% yield, based on Cu). Anal. calcd (%) for $\text{C}_{16}\text{H}_{12}\text{Br}_4\text{Cu}_2\text{N}_8\text{O}_2\text{S}_2$: C, 22.36; H, 1.41; N, 13.04; S, 7.45. Found (%): C, 22.28; H, 1.59; N, 12.98; S, 7.38%. IR selected data (KBr, cm^{-1}): 1660 (vs), 1654 (vs), 1601 (vs), 1559 (vs), 1526 (vs), 1495 (vs), 1442 (vs), 1407 (vs), 1222 (s), 1163 (s), 785 (m), 663 (m), 626 (m).

*Solvothermal Synthesis of $[\text{Cu}_3(\text{pymS})_2]_n$ (**3**), $[\text{Cu}(\text{pym}_2\text{S}_3)]_n$ [$\text{pym}_2\text{S}_3 = \text{Bis}(2\text{-pyrimidyl})\text{trisulfide}$] (**4**), and $[\text{Cu}_3\text{Br}(\text{pymS})_2]_n$ (**5**).*

All of the syntheses were carried out following the procedure above-mentioned for the isolation of **1**. The used solvents and reagents are as follows.

Synthesis of **3 and **4**.** Compound **3** was obtained by mixing CuI (99 mg, 0.52 mmol) and pym_2S_2 (115 mg, 0.52 mmol) in 26 mL of a $\text{H}_2\text{O}:\text{CH}_3\text{CN}$ mixture (3:10 in volume), as large light red block crystals. Yield (63 mg, 68%). Anal. calcd (%) for $\text{C}_8\text{H}_6\text{Cu}_3\text{IN}_4\text{S}_2$ (**3**): C, 17.73; H, 1.49; N, 10.34; S, 11.81. Found (%): C, 17.78; H, 1.52; N, 10.27; S, 11.35. IR (KBr, cm^{-1}): 1551 (s), 1365 (vs), 1172 (s) 820 (m), 745 (m), 669 (m). Besides the light red blocks, yellow crystals of 2-(pyrimidin-2-ylamino)-1,3-thiazole-4-carbaldehyde) previously synthesized by us²⁴ were also obtained (6 mg, 6% yield). After these crystals were removed, the mother solution was allowed to stand at room temperature for 2 weeks to yield crystals of **4** (12 mg, 5% yield). Anal. calcd (%) for $\text{C}_8\text{H}_6\text{CuIN}_4\text{S}_3$ (**4**): C, 21.60; H, 1.36; N, 12.60; S, 21.58. Found (%): C, 21.23; H, 1.41; N, 12.65; S, 21.55. IR (KBr, cm^{-1}): 3058 (w), 3043 (w), 1565 (s), 1550 (s), 1378 (s), 1163 (s), 817 (m), 759 (m), 743 (m), 640 (m), 468 (m).

Synthesis of **5.** This compound was prepared by mixing CuBr_2 (116 mg, 0.52 mmol) and pym_2S_2 (115 mg, 0.52 mmol) in 26 mL of a $\text{H}_2\text{O}:\text{CH}_3\text{CN}$ mixture (3:10 in volume) resulting in the formation of red crystals of **5** (53 mg, 62% yield based on Cu) together with the yellow $[\text{Cu}_3(\text{pymS})_3]_n$ compound⁴¹ (33 mg, 18%) and 2-(pyrimidin-2-ylamino)-1,3-thiazole-4-carbaldehyde)²⁴ (8 mg, 7% yield). Anal. calcd (%) for $\text{C}_8\text{H}_6\text{Cu}_3\text{BrN}_4\text{S}_2$ (**5**): C, 19.41; H, 1.63; N, 11.33; S, 12.93. Found (%): C, 19.53; H, 1.68; N, 11.28; S, 12.87. IR (KBr, cm^{-1}): 3060 (w), 3039 (w), 1557 (s), 1544 (s), 1371 (s), 1171 (s), 795 (m), 789 (m), 760 (m), 748 (m), 741 (m). When the solution was allowed to stand at 0 °C for 1 week, brown crystals of **2** were isolated (8 mg, 7% yield).

*Solvothermal Synthesis of $[\text{Cu}_2\text{I}_2(\text{pymSH})_2]_n$ (**6**) and $[\text{Cu}_2\text{I}_2(\text{pymSH})]_n$ (**7**).* A mixture of CuI (160 mg, 0.84 mmol) and pymSH (94 mg, 0.84 mmol) was stirred for 30 min in 28 mL of a $\text{CH}_2\text{Cl}_2:\text{CH}_3\text{CN}$ mixture (1:1 in volume), sealed in a 45 mL Teflon-lined autoclave, and heated at 90 °C for 20 h. Then, the solution was slowly cooled to room temperature during 26 h (2.5 °C/h). Small dark red crystals of **6** were obtained. Yield (189 mg, 74%). Anal. calcd (%) for $\text{C}_8\text{H}_8\text{Cu}_2\text{I}_2\text{N}_4\text{S}_2$ (**6**): C, 15.87; H, 1.33; N, 9.26; S, 10.57. Found (%): C, 15.11; H, 1.35; N, 9.18; S, 10.34. IR (KBr, cm^{-1}): 3215 (w), 3106 (w), 1603 (s), 1576 (s), 1506 (m), 1481 (m) 1460 (m), 1421 (m), 1336 (m), 1319 (m), 1175 (s), 1107 (s), 1084 (s), 1058 (s), 1015 (m), 793 (m), 742 (m), 462 (m).

Square planar red crystals of compound **7** were isolated by using a Cu: pymSH molar ratio of 2:1 instead of 1:1; that is, by mixing CuI (160 mg, 0.84 mmol) and pymSH (63 mg, 0.56 mmol) in 28 mL of a $\text{CH}_2\text{Cl}_2:\text{CH}_3\text{CN}$ mixture (1:1 in volume). Yield (210 mg, 76%). Anal. calcd (%) for $\text{C}_4\text{H}_4\text{Cu}_2\text{I}_2\text{N}_2\text{S}$ (**7**): C, 9.74; H, 0.82; N, 5.68; S, 6.50. Found (%): C, 9.62; H, 0.85; N, 5.71; S, 6.43. IR (KBr, cm^{-1}): 3215 (w), 3106 (w), 1603 (s), 1576 (s), 1506 (m), 1481 (m) 1460 (m), 1421 (m), 1336 (m), 1319 (m), 1175 (s), 1107 (s), 1084 (s), 1058 (s), 1015 (m), 793 (m), 742 (m), 462 (m).

RESULTS AND DISCUSSION

The solvothermal reaction (90 °C/20 h) between CuI and bis(2-pyrimidyl)disulfide (pym_2S_2) in a 1:1 ratio in volume and in $\text{CH}_2\text{Cl}_2:\text{CH}_3\text{CN}$ leads to the formation of the coordination

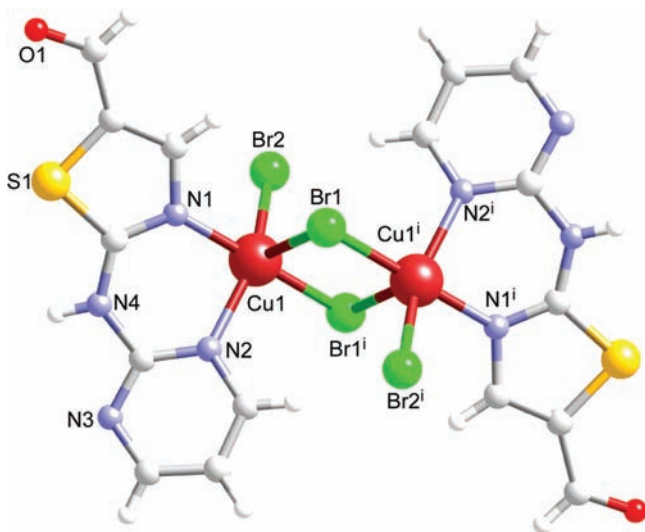
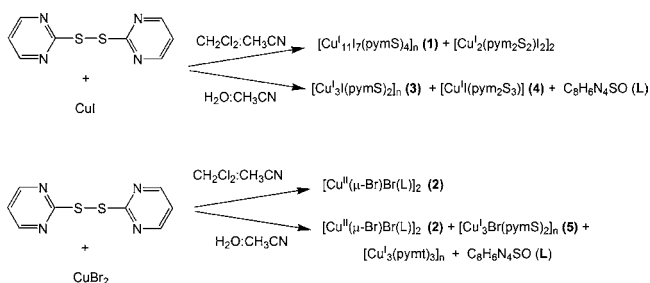
Scheme 1. Schematic Synthetic Procedures from pym_2S_2 [L = 2-(Pyrimidin-2-ylamino)-1,3-thiazole-4-carbaldehyde]

Figure 1. View of the dimeric entity in compound **2** showing the atom-labeling scheme.

Table 2. Selected Bond Distances (Å) and Angles for Compound 2^a

atoms	distance	atoms	angle
Cu1–N1	1.978(5)	N1–Cu1–N2	86.8(2)
Cu1–N2	2.081(5)	N1–Cu1–Br1	91.68(15)
Cu1–Br1	2.6788(12)	N1–Cu1–Br2	89.19(16)
Cu1–Br2	2.4448(11)	N1–Cu1–Br1 ⁱ	176.26(15)
Cu1–Br1 ⁱ	2.3874(11)	N2–Cu1–Br1	104.52(14)
Cu1...Cu1 ⁱ	3.5299(17)	N2–Cu1–Br2	151.28(15)
		N2–Cu1–Br1 ⁱ	93.44(15)
		Br1–Cu1–Br2	104.02(4)
		Br1–Cu1–Br1 ⁱ	91.86(4)
		Br1 ⁱ –Cu1–Br2	88.80(4)
		Cu1–Br1–Cu1 ⁱ	88.14(4)

^aSymmetry code: (i) $-x + 1, -y, -z$.

polymer $[\text{Cu}_{11}\text{I}_7(\text{pymSH})_4]_n$ (**1**), in high yield. This compound has been recently obtained, as a byproduct (in low yield), by reacting $\text{CuSO}_4 \cdot 5\text{H}_2\text{O}$, pyrimidine-2(1H)-thione (pymSH), KI, and NH_4SCN (2:1:2:2 molar ratio) under more energetic solvothermal conditions (140 °C, 96 h).⁴² The development of an alternative synthetic procedure for this compound, in higher yields, is especially valuable to study its interesting physical properties in solid state (see below). Remarkably, isolation of crystals of **1** from the direct reaction of a copper(I) halide is a very unusual synthetic procedure since it typically produces the fast precipitation of insoluble products. However, the analogous

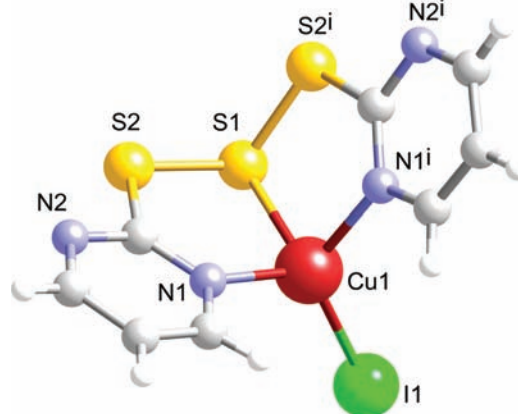

Figure 2. View of the monomeric entity in compound **4**.

Table 3. Selected Bond Distances (Å) and Angles for Compound 4^a

atoms	distance	atoms	angle
Cu1–N1	2.053(2)	N1–Cu1–N1 ⁱ	101.25(13)
Cu1–N1 ⁱ	2.053(2)	N1–Cu1–S1	91.54(8)
Cu1–S1	2.3490(11)	N1–Cu1–I1	124.25(6)
Cu1–I1	2.4967(7)	N1 ⁱ –Cu1–S1	91.53(8)
		N1 ⁱ –Cu1–I1	124.25(6)
		S1–Cu1–I1	115.05(3)

^aSymmetry code: (i) $x, -y + 1/2, z$.

reaction using CuBr_2 instead of CuI leads to the formation of a brown crystalline solid characterized as $[\text{Cu}^{\text{II}}(\mu\text{-Br})(\text{Br})\text{L}]_2$ [L = 2-(pyrimidin-2-ylamino)-1,3-thiazole-4-carbaldehyde] (**2**), in high yield (Scheme 1). In both solvothermal reactions, pale yellow orthorhombic crystals of elemental sulfur S_8 were formed in traces amount [crystal data for S_8 : orthorhombic, space group $Fddd$, $a = 10.464(4)$ Å, $b = 12.851(5)$ Å, $c = 24.51(1)$ Å, $V = 3296(2)$ Å³]. Sulfur formation can be rationalized taking into account that the formation of **1** implies cleavage of a S–S and a S–C(sp²) bond and the formation of **2** implies the cleavage of three bonds, S–S, S–C(sp²), and N–C(sp²) in the pym_2S_2 ligand. Although the S–S bond cleavage in dithiodipyrindine is common under solvothermal conditions, the C–S bond cleavage is much less frequent,^{2,33,43} and the in situ multiple bond cleavage of S–S, S–C(sp²), and N–C(sp²) has been only recently reported by us in the solvothermal reaction between CuCl_2 and (pym_2S_2) .²⁴

The inspection by ESI-MS spectrometry of all of the solutions obtained in both solvothermal reactions between Cu(I/II) and pym_2S_2 shows three peaks at m/z 223.01, 191.04, and 159.07, corresponding to the monoprotonated cations of the pym_2S_2 , pym_2S , and 2,2'-bipym entities, respectively, and three peaks at m/z 252.96, 284.93, and 317.08 corresponding to the radical cations $[\text{Cu}(\text{pym}_2\text{S})]^{\bullet+}$, $[\text{Cu}(\text{pym}_2\text{S}_2)]^{\bullet+}$, and $[\text{Cu}(\text{pym}_2\text{S}_3)]^{\bullet+}$, respectively. These data, together with the formation of S_8 , suggest that in a first step the homolytic rupture of the S–S and S–C(sp²) bonds and subsequent formation of free radical intermediates $[\text{pymS}]^{\bullet}$, $[\text{pymS}]^{\bullet}$, and $[2\text{-pym}]^{\bullet}$ could take place, followed by self-recombination of these radicals. Additionally, it is probably that part of the S^{\bullet} radicals self-recombine to give the observed S_8 . The formation of **2** implies the additional cleavage of the N–C(sp²) bond, which could take place with the in situ-generated pyrimidine-2-thione. The facility of pyrimidine-2-thione to form compound **2**

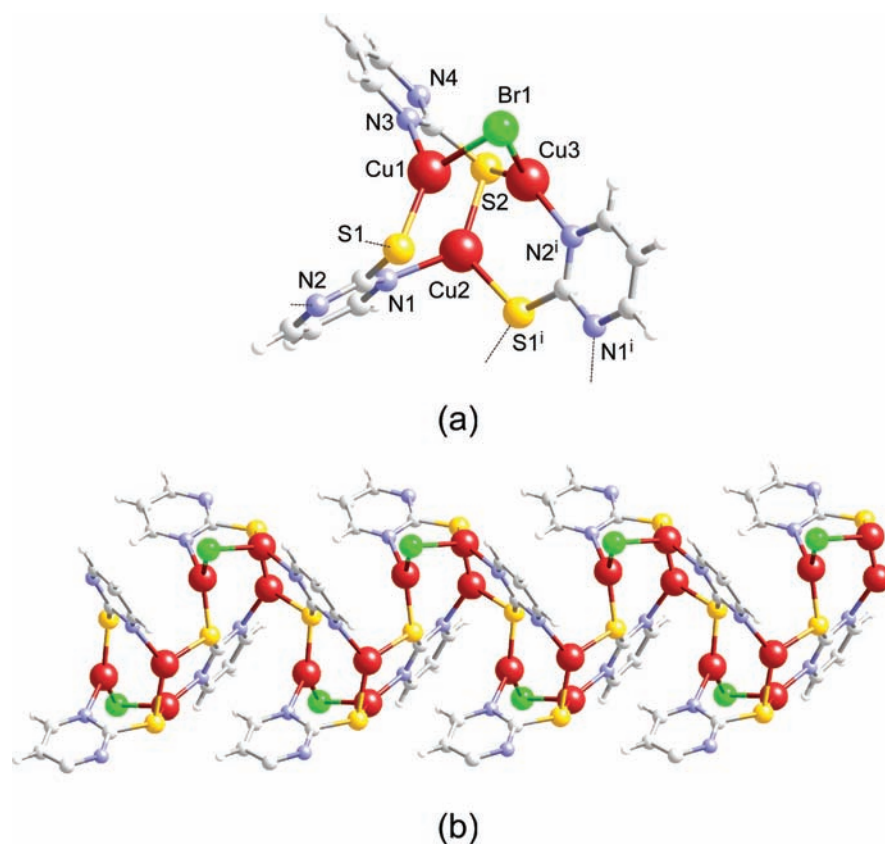


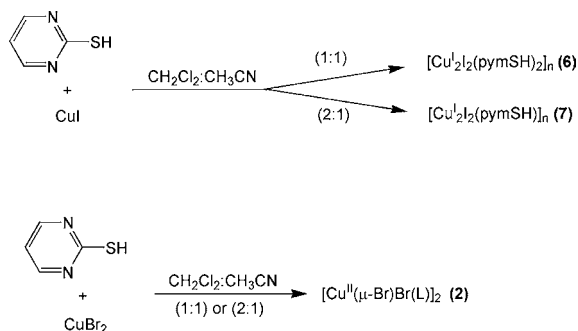
Figure 3. Coordination environments of copper sites (a) and the helical chain of 5 (b).

Table 4. Selected Bond Distances (Å) and Angles for Compound 5^a

atoms	distance	atoms	angle
Cu1–N3	1.989(4)	N3–Cu1–S1	135.72(12)
Cu1–S1	2.1841(14)	N3–Cu1–Br1	105.47(12)
Cu1–Br1	2.4541(8)	S1–Cu1–Br1	118.39(4)
Cu2–N1	2.033(4)	N1–Cu2–S1 ⁱ	106.71(12)
Cu2–S1 ⁱ	2.2855(14)	N1–Cu2–S2	128.88(12)
Cu2–S2	2.2506(14)	S1 ⁱ –Cu2–S2	123.41(5)
Cu3–N2 ⁱ	2.006(4)	N2 ⁱ –Cu3–S2	137.87(13)
Cu3–S2	2.2060(14)	N2 ⁱ –Cu3–Br1	97.60(13)
Cu3–Br1	2.5484(8)	S2–Cu3–Br1	122.16(4)
Cu1...Cu2	2.9897(9)	Cu1...Cu2...Cu3	53.53(2)
Cu1...Cu3	2.5923(10)	Cu2...Cu1...Cu3	58.44(2)
Cu2...Cu3	2.7468(9)	Cu1...Cu3...Cu2	68.04(3)

^aSymmetry code: (i) $-x + 1, y + 1/2, -z + 3/2$.

Scheme 2. Schematic Synthetic Procedures from pymSH



has been also observed in the reaction between CuBr_2 and pyrimidine-2-thione in 1:1 or 2:1 molar ratios under similar solvothermal conditions ($\text{CH}_2\text{Cl}_2:\text{CH}_3\text{CN}$, 90 °C, 20 h), where 2 was obtained from the solution.

Compound 2 is isostructural to a chloride Cu(II) analog, previously reported by us.²⁴ Its crystal structure consists of centrosymmetric double bromido-bridged copper(II) dimeric entities. The in situ-formed 2-(pyrimidin-2-ylamino)-1,3-thiazole-4-carbaldehyde molecule is coordinated to the metal center through N1 and N2 nitrogen atoms to form a six-membered chelating ring. The value of the bite angle is 86.8(2)°. Two bridging and one terminal bromide anions are also coordinated to the metal center and complete the CuBr_3N_2 coordination environment. The bridging bromide anions are coordinated to the two copper atoms in an asymmetric fashion with significantly different bond lengths, 2.3874(11) and 2.6788(12) Å, caused by the active Jahn–Teller distortion of the copper(II) ion. A drawing of the dimer structure showing the labeling scheme is given in Figure 1. Selected bond lengths and angles are reported in Table 2.

The penta-coordination of Cu(II) is rather common and usually presents either a square-pyramidal or a trigonal-bipyramidal geometry (or any of the distorted intermediate geometries). The geometry of the CuBr_3N_2 chromophore can be quantitatively characterized using the parameter τ , as defined by Addison et al.⁴⁴ The calculated value of $\tau = 0.42$ (relative to one for a regular trigonal bipyramid and zero for a square pyramid) indicates that the coordination geometry around the metal center, although intermediate between the two ideal polyhedrons, is closer to an elongated tetragonal pyramid with the bromide anions placed alternatively on equatorial and apical positions. As a result, the geometry of the complex consists of

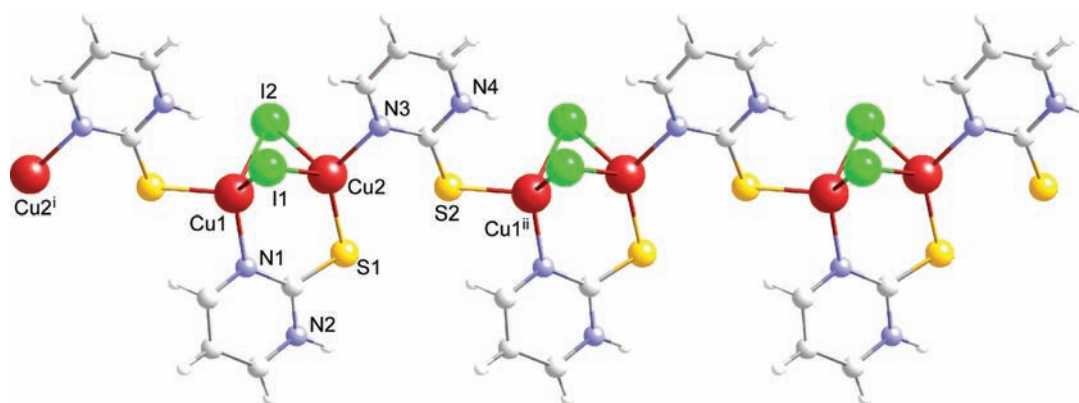


Figure 4. Almost linear chain of compound 6.

Table 5. Selected Bond Distances (Å) and Angles for Compound 6^a

atoms	distance	atoms	angle
Cu1–N1	2.062(4)	N1–Cu1–S2	102.67(11)
Cu1–S2	2.2780(12)	N1–Cu1–I1	108.68(11)
Cu1–I1	2.6368(7)	N1–Cu1–I2	125.00(11)
Cu1–I2	2.7249(6)	S2–Cu1–I1	114.83(4)
		S2–Cu1–I2	103.78(4)
		I1–Cu1–I2	102.39(2)
Cu2–N3	2.040(4)	N3–Cu2–S1	122.69(11)
Cu2–S1	2.2329(12)	N3–Cu2–I1	95.87(11)
Cu2–I1	2.9041(7)	N3–Cu2–I2	103.04(11)
Cu2–I2	2.6576(7)	S1–Cu2–I1	109.01(4)
		S1–Cu2–I2	122.78(4)
		I1–Cu2–I2	102.39(2)
Cu1...Cu2	2.5950(8)	Cu2...Cu1...Cu2 ⁱ	163.22(3)
Cu1...Cu2 ⁱ	5.5639(9)	Cu1...Cu2...Cu1 ⁱⁱ	163.22(3)

^aSymmetry code: (i) $x - 1, y + 1, z$; (ii) $x + 1, y - 1, z$.

two square pyramids sharing one base-to-apex edge, with parallel basal planes.^{45–47} The copper atom is displaced from the mean equatorial plane toward the corresponding axial bromido bridging atoms by 0.311 Å.

Within the $\text{Cu}(\mu\text{-Br})_2\text{Cu}$ core, the $\text{Cu}\cdots\text{Cu}$ distance is 3.523(2) Å, and the Cu_2Br_2 core presents an almost ideal rectangular geometry as indicated by the $\text{Br}-\text{Cu}-\text{Br}$ and $\text{Cu}-\text{Br}-\text{Cu}$ bond angles of 88.14(4) and 91.86(4)°, respectively.

Table 6. Selected Bond Distances (Å) and Angles for Compound 7^a

atoms	distance	atoms	angle
Cu1–N1	2.054(5)	N1–Cu1–I1	113.18(13)
Cu1–I1	2.6571(8)	N1–Cu1–I1 ⁱ	111.01(13)
Cu1–I1 ⁱ	2.6681(8)	N1–Cu1–I2	102.82(14)
Cu1–I2	2.7435(9)	I1–Cu1–I1 ⁱ	120.40(3)
		I1–Cu1–I2	109.69(3)
		I1 ⁱ –Cu1–I2	97.02(3)
Cu2–S1 ⁱ	2.3309(16)	S1 ⁱ –Cu2–S1 ⁱⁱⁱ	93.55(5)
Cu2–S1 ⁱⁱ	2.3707(15)	S1 ⁱ –Cu2–I1	115.01(5)
Cu2–I1	2.5829(8)	S1 ⁱ –Cu2–I2	107.80(5)
Cu2–I2	2.5525(8)	S1 ⁱⁱ –Cu2–I1	109.64(5)
		S1 ⁱⁱⁱ –Cu2–I2	109.30(5)
		I1–Cu2–I2	118.60(3)
Cu1...Cu1 ⁱ	2.6463(14)	Cu1 ⁱ ...Cu1...Cu2	74.63(3)
Cu1...Cu2	2.7032(10)	Cu1...Cu2...Cu2 ⁱⁱⁱ	161.77(4)
Cu2...Cu2 ⁱⁱⁱ	3.2200(15)		

^aSymmetry code: (i) $-x + 1, -y + 2, -z + 2$; (ii) $x, y + 1, z$; (iii) $-x + 1, -y + 3, -z + 2$.

The dimeric entities assemble together by means of $\text{N}-\text{H}\cdots\text{Br}$ hydrogen bonds to give rise to 1D supramolecular chains, which are further connected through weak $\text{C}-\text{H}\cdots\text{N/O}$ hydrogen bonds to provide the overall 3D cohesiveness to the crystal structure. No evidence of $\text{Br}\cdots\text{Br}$ contacts have been observed. The structure of compound 3, previously reported,⁴² is comprised of 2-fold screw chains in which helical chains

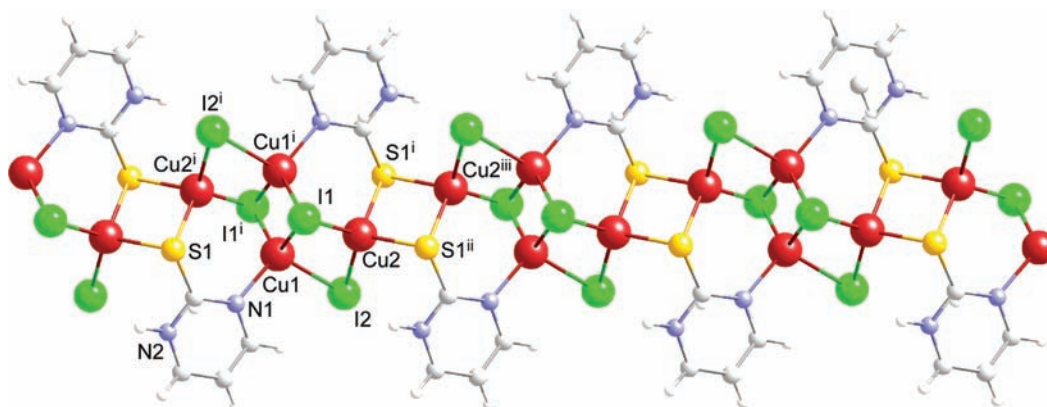


Figure 5. Fragment of the 1D coordination polymer of compound 7.

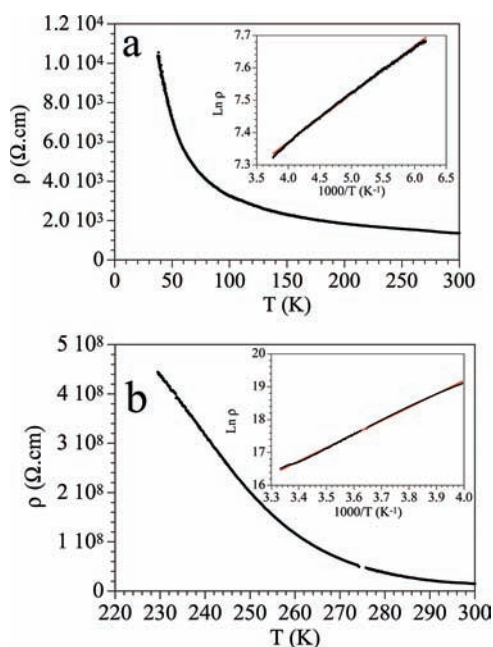


Figure 6. Thermal variation of the electrical resistivity of **3** (a) and **5** (b). The insets show the Arrhenius plots showing the semiconducting behavior.

Table 7. Selected Luminescent Properties of the Cu(I) Compounds

compd	$\lambda_{\text{max}}^{\text{emi}}$ (nm)
1	626, 652, 670, 686, 712, 734, 762
3	624, 648, 668, 683, 710, 731, 762
5	621, 653, 670, 688, 716, 737, 769
6	689, 713, 734, 764
7	672, 685, 711, 732, 762

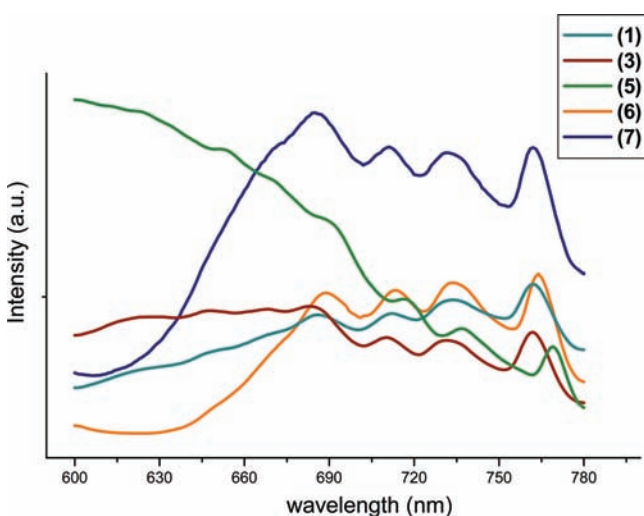


Figure 7. Emission spectra of **1** (blue line), **3** (brown line), **5** (green line), **6** (orange line), and **7** (violet line) in the solid state at 450 nm.

$[\text{Cu}_3(\text{pymS})_2]_n^{n+}$ are connected through iodides attached to the metal centers.

On the other hand, it is well-known that the products under hydro(solvo)thermal conditions can be influenced by some parameters such as solvent, temperature, and so on. To examine the role of solvent in these processes, a similar reaction

was carried out in $\text{H}_2\text{O}:\text{CH}_3\text{CN}$ (3:10 in volume), leading to the formation of $[\text{Cu}_3\text{I}(\text{pymS})_2]_n$ (**3**) as the sole compound. The synthesis of **3** has been previously reported, but in that reaction, this coordination polymer crystallized together with **1**.⁴² Additionally, single crystals of $[\text{CuI}(\text{pym}_2\text{S}_3)]$ (**4**) are isolated from the mother solution after filtration of **3**. The formation of **4** represents the second reported example of transformation of a bis(2-pyrimidyl)disulfide to a polysulfide compound, as we have previously reported a copper(II) compound with the pym_2S_3 ligand²⁴ (Scheme 1).

Compound **4** consists of neutral monomeric $[\text{Cu}(\text{pym}_2\text{S}_3)\text{I}]$ entities, in which the copper(I) center is placed in a distorted tetrahedral surrounding coordinated to two nitrogen atoms and the central sulfur atom of the pym_2S_3 ligand and a iodide anion (Figure 2). Selected bond distances and angles are gathered in Table 3. The overall 3D cohesiveness of the crystal structure is ensured by the presence of C–H \cdots N hydrogen-bonding interactions among the pym_2S_3 [$\text{C}3\cdots\text{N}2 = 3.541(4)$ Å, $\text{C}3\text{–H}\cdots\text{N}2 = 176^\circ$]^{48–52} and S \cdots S contacts (3.193(1) Å) among the coordinated and noncoordinated sulfur atoms and also by unusual C–H \cdots I hydrogen-bonding interactions [$\text{C}4\cdots\text{I}1 = 3.976(3)$ Å, $\text{C}4\text{–H}\cdots\text{I}1 = 151^\circ$].

It is worth mentioning that coordination polymers based on copper(I) halide as building blocks or secondary building units (SBU) have been revised recently and are a subject of continuous interest in crystal engineering.^{52–56}

The analogous solvothermal reaction carried out with CuBr_2 , instead of CuI , leads to formation of **5**. Compound **5** is isostructural with **3** but replaces the iodide anions by bromides. The $\mu_3\text{–}1\kappa\text{N}:2,3\kappa\text{S}$ and $\mu_4\text{–}1\kappa\text{N}:2,3\kappa\text{S}:4\kappa\text{N}$ coordination mode of the pymS ligands generates helical $[\text{Cu}_3(\text{pymS})_2]_n^{n+}$ chains (Figure 3) that are further connected by means of bridging bromide anions to provide a final 3D coordination polymer. There are three crystallographically independent copper(I) centers, two pymS ligands and one bromide anion. The Cu2 atom is coordinated by two sulfur atoms and one nitrogen atom from three pymS ligands in a trigonal planar arrangement. A semicoordination interaction with the nitrogen atom of a fourth pymS ligand is also observed [$\text{Cu}1\cdots\text{N}4 = 2.495(5)$ Å]. The Cu1 and Cu3 atoms show similar coordination environments: They are coordinated by a bridging bromide and by a nitrogen and a sulfur atom from two different pymS ligands. Selected bond distances and angles are listed in Table 4. The Cu(I) ions are alternately bridged by pymS ligands to form a cationic helical chain of $[\text{Cu}_3(\text{pymS})_2]_n^{n+}$ in which adjacent Cu(I) ions are arranged into a Cu_3 trimer with short Cu \cdots Cu distances (Table 4). The neutrality of the chain is achieved with μ_2 bromido bridges connecting Cu1 and Cu3 atoms (Figure 3b). Adjacent helical chains are packed via Cu \cdots N ($\text{Cu}2\cdots\text{N}4 = 2.495$ Å), Cu \cdots Br ($\text{Cu}3\cdots\text{Br}1 = 3.085$ Å), and S \cdots S ($\text{S}2\cdots\text{S}2 = 3.491$ Å) weak interactions into a 3D supramolecular array in which two adjacent helical chains are parallel and heterochiral.

Finally, the reactions between Cu^{I} and pyrimidine-2-thione in 1:1 or 2:1 ratio under solvothermal conditions in $\text{CH}_2\text{Cl}_2:\text{CH}_3\text{CN}$ (1:1, in volume) lead to the formation of the polymers **6** and **7**, respectively (Scheme 2). To form **6** and **7** as sole compounds, it is necessary to properly adjust the concentrations of the reactants. We have observed that other concentrations different to those used in the Experimental Section lead to mixtures of both compounds.

The crystal structures of compounds **6** and **7** are conditioned by the nondeprotonation of the pymSH ligand that limits its denticity. The ligand shows the thione tautomeric form with

the acidic proton placed in one of the nitrogen atoms. Therefore, it becomes a bidentate ligand with a potential coordination ability reduced to the sulfur and one of the two nitrogen atoms. Both crystal structures consist of polymeric linear chains in which bridging pymSH and iodide anions coexist.

In compound **6**, the chains can be described as $[\text{Cu}_2\text{I}_2(\text{pymSH})]$ dimers that are connected by a second pymSH ligand (Figure 4), giving rise to two different intrachain Cu...Cu distances: 2.5949(8) Å within the dimer and 5.5639(9) Å between adjacent dimers. The iodide anions adopt a μ_2 coordination mode, and the two crystallographically independent pymSH ligands present very similar bridging coordination modes ($\mu_2\text{-}1\kappa\text{N:}2\kappa\text{S}$ and $\mu_2\text{-}1\kappa\text{S:}2\kappa\text{N}$ for the intra- and interdimer bridges, respectively). The chain cohesion is also reinforced by the presence of intrachain S...S contacts [$\text{S}1\cdots\text{S}2 = 3.3507(15)$ Å] and a hydrogen bond established between the protonated N atom and one of the bridging iodides [$\text{N}4\cdots\text{I}1 = 3.610(4)$ Å, $\text{N}4\text{-H}\cdots\text{I}1 = 143(6)^\circ$]. The two copper(I) ions present very similar tetrahedral coordination environments with a I_2NS donor set. Selected bond distances and angles are gathered in Table 5.

The packing of the chains is mainly due to N-H...I hydrogen bonds [$\text{N}2\cdots\text{I}1 = 3.479(4)$ Å, $\text{N}2\text{-H}\cdots\text{I}1 = 139(5)^\circ$] and $\pi\text{-}\pi$ interactions (closest contacts: 3.29–3.40 Å) between the aromatic ring of the pymSH ligands, but there are also evidence of nonusual C-H...I hydrogen-bonding interactions [$\text{C}2\cdots\text{I}2 = 3.698(5)$ Å, $\text{C}2\text{-H}\cdots\text{I}2 = 121(4)^\circ$; $\text{C}6\cdots\text{I}2 = 3.875(5)$ Å, $\text{C}6\text{-H}\cdots\text{I}2 = 154(5)^\circ$].

The polymeric chain of compound **7** is composed of compact $[\text{Cu}_4\text{I}_4]$ clusters that are linked through pymSH bridges (Figure 5). This type of ladderlike motif is quite common for coordination polymers containing Cu(I)–I SBUs.⁵⁴ The lower pymSH/Cu ratio as compared with **6** leads to an increase of the metal centers coordinated to both the iodide anions and the pymSH ligand. In that way, some of the iodide anions adopt the μ_3 -coordination mode and that of the pymSH ligand becomes $\mu_3\text{-}1\kappa\text{N:}2,3\kappa\text{S}$. The two crystallographically independent copper(I) ions present tetrahedral coordination environments but different donor sets: I_3N for Cu1 and I_2S_2 for Cu2. Selected bond distances and angles are gathered in Table 6.

The N-H group of the pymSH ligand establishes a bifurcated hydrogen bond with two iodides [$\text{N}2\cdots\text{I}1 = 3.594(5)$ Å, $\text{N}2\text{-H}\cdots\text{I}1 = 132.2^\circ$; $\text{N}2\cdots\text{I}2 = 3.538(5)$ Å, $\text{N}2\text{-H}\cdots\text{I}2 = 121.3^\circ$]. One of them belongs to the same polymeric chain and reinforces in this way the intrachain cohesiveness. The second one involves an adjacent chain and, altogether with $\pi\text{-}\pi$ interactions (closest contacts: 3.31–3.55 Å) and some weak C-H...I hydrogen bonds [$\text{C}1\cdots\text{I}2 = 3.842(6)$ Å, $\text{C}1\text{-H}\cdots\text{I}2 = 138.1^\circ$] is responsible of the 3D cohesiveness.

As we have already mentioned in the Introduction, coordination polymers may present a variety of physical properties. In particular, those containing copper(I) and organosulfur ligands may exhibit interesting electrical and/or optical properties. This can be rationalized taking into account that the incorporation of thiolate-S as a bridge between adjacent transition metal sites in coordination polymers is highly desirable in terms of electronic (magnetism, conductivity) and luminescent properties, since the metal orbital energies are better matched for sulfur and a larger delocalization of spin density toward the bridging atom can be achieved.³²

Specifically, we have recently reviewed aspects concerning the electrical conductivity in coordination polymers showing that those coordination polymers formed by Cu(I) and Cu(I,II) centers bridged by sulfur-containing ligands are especially good electrical conductors.³⁰ Therefore, we have studied the electrical properties of compounds **1**, **3**, and **5–7** since their structures show some of the desirable structural features mentioned before.

In a first test, we have used a setup based on the two contacts method. For this instrumental option, we take a single crystal that is connected by two tungsten tips. A voltage ramp between -10 V and $+10$ V is then applied to the tungsten tips at room temperature (300 K), and simultaneously, we record the electrical current that passes through the crystal as a consequence of the voltage difference. Taking into account the geometrical parameters of the crystal, these measurements together with Ohm's law allow us to determine the conductivity. We repeat all of this procedure with several crystals for each compound, and the final conductivity value is given by the average value. For the case of the complexes **1**, **6**, and **7**, the electrical conductivity so determined is smaller than 10^{-9} S cm^{-1} . This conductivity is quite low so we can consider them as insulators.

However, compounds **3** and **5** exhibit conductivity values in the order of magnitude of 10^{-6} and 10^{-7} S cm^{-1} , respectively. These values suggest a semiconductor behavior of these compounds. To get more information of such complexes, we have also performed dc electrical conductivity measurements with the four contacts method as a function of the temperature. The conductivity values at 300 K for compounds **3** and **5** measured with the four contacts method are ca. 7×10^{-4} and 6×10^{-8} S cm^{-1} , respectively. In the case of **3**, the much higher value observed with the four contacts method is probably due a better quality of the crystals since both methods give similar results when the resistance of the samples is high, as in compounds **3** and **5**. In both compounds, the thermal variation of the electrical conductivity shows an exponential increase of the resistivity as the temperature is decreased (Figure 6), showing a semiconducting behavior that follows the Arrhenius law, $\rho = \rho_0 \exp(E_a/kT)$. At temperatures below ca. 50 (in **3**) and 230 K (in **5**), the resistance of the sample becomes too high to be measured by our equipment. The Arrhenius plot of the thermal variation of the resistivity (inset of Figure 6) allows us to determine activation energies of ca. 13 and 400 meV for compounds **3** and **5**, respectively. Because both compounds are isostructural and only differ in the bridging halogen atom (I in **3** and Br in **5**), we can explain the higher conductivity value and the lower activation energy of compound **3** as a logical consequence of the higher overlap of the iodine bridges as compared with the bromine ones. Note that these effects (increase of the conductivity and decrease of the activation energy) have been observed in other cases when bromine bridges are replaced by iodine ones.³⁰

Coordination polymers with aromatic ligands and d^{10} metal centers are very likely to exhibit fluorescence/luminescence.^{57,58} Therefore, the luminescent properties of Cu(I) compounds (**1**, **3**, and **5–7**) were investigated in the solid state, since the preparation of solutions was precluded by their insolubility. At room temperature, excitation of solid samples at $\lambda = 420$ nm produces an intense red emission with several peaks and maximum values centered at 762, 683, 621, 764, and 685 nm, respectively (Table 7 and Figure 7).

In general, possible assignments for the excited states that are responsible for emission phenomena of Cu(I) complexes are ligand-centered $\pi \rightarrow \pi^*$ transitions (LC), ligand-to-ligand (LLCT), ligand-to-metal (LMCT), or metal-to-ligand (MLCT) charge-transfer transitions or metal-centered $d^{10} \rightarrow d^9s^1$ (MCC) transitions.⁵⁹ An assignment of ligand-centered $\pi \rightarrow \pi^*$ and/or intraligand transitions can be excluded on the basis of the emission of free ligands pymSH and pym₂S₂, which display weak emission in the solid state with a high-energy band around 350–550 and 460–550 nm, respectively. By comparison with other organic luminescent compounds, these bands probably come from the fluorescence of (π , π^*) excited states.⁶⁰ Also, the π^* orbitals for the thiolate ligands are too high to justify a MLCT assignment for the lowest-lying excited state.⁶¹

According to the photoluminescent properties of other Cu(I)/halide/thiolate clusters, these low-energy red emissions in compounds **1**, **3**, and **5–7** are due to a triplet “cluster-centered” (CC) excited state and might be assigned to a combination of iodide-to-metal charge transfer (LMCT), metal-to-iodide charge transfer (MLCT), and/or metal cluster-centered transitions [MCC, dCu \rightarrow (s,p)Cu] in orbital parentage.^{41,59,61–64} The existence of a MCC contribution is supported by short Cu–Cu distances [2.6681(9)–2.7138(12) Å], less than twice the van der Waals radius of Cu (i.e., less than 2.8 Å), consistent with the previous reported results for Cu_xI_y clusters.^{65,66} In contrast, a compound where the Cu–Cu distance is substantially longer than 2.8 Å is not emissive due to its very weak Cu–Cu interaction.⁶⁴ This means that the Cu–Cu distance plays a key role in the photoluminescence of Cu(I) complexes. The **1**, **3**, **6**, and **7** complexes show very similar emission spectra, suggesting that the transitions are localized on the Cu_nI_m cluster and are essentially independent of the ligand. The low-energy luminescence observed at ca. 760 nm are unusual and are quite different to the large numbers of blue emission coordination polymers,⁶⁷ representing, thus, one of the lowest energy emissions, to our knowledge, in luminescent d¹⁰ transition-metal complexes to date, although some examples of polynuclear Cu(I)–organosulfur compounds showing NIR luminescence have been recently published.^{41,68}

CONCLUSIONS

The results reported here suggest that the use of solvothermal methods allows the formation of a variety of copper coordination polymers of different architectures and functionalities. The coexistence in a coordination polymer of copper- and sulfur-containing ligands, seems to be especially suitable toward the formation of materials with interesting electronic properties. Thus, polymers **3** and **5** comprise two unusual physical properties: They show high electrical conductivity values and strong luminescent red emissions, both at room temperature. The low-energy luminescence observed at ca. 760 nm is one of the lowest energy emissions, to our knowledge, in luminescent d¹⁰ transition-metal complexes to date, which provides potential candidates for practical applications as electronic and optical devices.

Additionally, it is worth to mention that the C–S and S–S bonds cleavage and reorganization observed in these synthesis open new perspectives toward the development of alternative routes for the synthesis of organic ligands and may be potentially relevant in processes such as petroleum-chemical hydrodesulfurization and bioorganic and bioinorganic chemistry.^{27,69}

ASSOCIATED CONTENT

Supporting Information

X-ray crystallographic files in CIF format. This material is available free of charge via the Internet at <http://pubs.acs.org>.

AUTHOR INFORMATION

Corresponding Author

*E-mail: felix.zamora@uam.es (F.Z.) or salome.delgado@uam.es (S.D.).

ACKNOWLEDGMENTS

This work was supported by the MICINN (MAT2010-20843-C02-01, MAT2008-05690/MAT, ACI2009-0969, and CTQ-2011-26507), Comunidad de Madrid (S-0505/MAT/0303), Gobierno Vasco (IT477-10), and the Generalitat Valenciana (Prometeo 2009/095).

REFERENCES

- (1) Kitagawa, S.; Noro, S. *In Comprehensive Coordination Chemistry II*; Elsevier: Amsterdam, 2004; Vol. 7.
- (2) Brammer, L. *Chem. Soc. Rev.* **2004**, *33*, 476–489.
- (3) Kitagawa, S.; Kitaura, R.; Noro, S. *Angew. Chem., Int. Ed.* **2004**, *43*, 2334–2375.
- (4) Hou, H. W.; Meng, X. R.; Song, Y. L.; Fan, Y. T.; Zhu, Y.; Lu, H. J.; Du, C. X.; Shao, W. H. *Inorg. Chem.* **2002**, *41*, 4068–4075.
- (5) Mas-Balleste, R.; Gomez-Herrero, J.; Zamora, F. *Chem. Soc. Rev.* **2010**, *39*, 4220–4233.
- (6) Mateo-Marti, E.; Welte, L.; Amo-Ochoa, P.; Miguel, P. J. S.; Gomez-Herrero, J.; Martin-Gago, J. A.; Zamora, F. *Chem. Commun.* **2008**, 945–947.
- (7) Olea, D.; Alexandre, S. S.; Amo-Ochoa, P.; Guijarro, A.; de Jesus, F.; Soler, J. M.; de Pablo, P. J.; Zamora, F.; Gomez-Herrero, J. *Adv. Mater.* **2005**, *17*, 1761–1765.
- (8) Welte, L.; Garcia-Couceiro, U.; Castillo, O.; Olea, D.; Polop, C.; Guijarro, A.; Luque, A.; Gómez-Rodríguez, J. M.; Gómez-Herrero, J.; Zamora, F. *Adv. Mater.* **2009**, *21*, 2025–2028.
- (9) Long, J. R.; Beauvais, L. G.; Shores, M. P. *J. Chem. Am. Soc.* **2000**, *122*, 2763–2772.
- (10) Mas-Balleste, R.; Gomez-Navarro, G.; Gomez-Herrero, J.; Zamora, F. *Nanoscale* **2011**, *3*, 20–30.
- (11) Chen, X. M.; Zhang, J. P.; Zheng, S. L.; Huang, X. C. *Angew. Chem., Int. Ed.* **2004**, *43*, 206–209.
- (12) Chen, X. M.; Tong, M. L. *Acc. Chem. Res.* **2007**, *40*, 162–170.
- (13) Ford, P. C.; Vogler, A. *Acc. Chem. Res.* **1993**, *26*, 220–226.
- (14) Raper, E. S. *Coord. Chem. Rev.* **1994**, *129*, 91–156.
- (15) Raper, E. S. *Coord. Chem. Rev.* **1996**, *153*, 199–255.
- (16) Raper, E. S. *Coord. Chem. Rev.* **1997**, *165*, 475–567.
- (17) Sousa, A.; Garcia-Vazquez, J. A.; Romero, J. *Coord. Chem. Rev.* **1999**, *193–5*, 691–745.
- (18) Akrivos, P. D. *Coord. Chem. Rev.* **2001**, *213*, 181–210.
- (19) Lobana, T. S.; Sharma, R.; Bermejo, E.; Castineiras, A. *Inorg. Chem.* **2003**, *42*, 7728–7730.
- (20) Feng, P. Y.; Han, L.; Bu, X. H.; Zhang, Q. C. *Inorg. Chem.* **2006**, *45*, 5736–5738.
- (21) Gou, S. H.; Huang, C. H.; Zhu, H. B.; Huang, W. *Inorg. Chem.* **2007**, *46*, 5537–5543.
- (22) Tong, M. L.; Wang, J.; Zhang, Y. H.; Li, H. X.; Lin, Z. J. *Cryst. Growth Des.* **2007**, *7*, 2352–2360.
- (23) Tong, M. L.; Wang, J.; Zheng, S. L.; Hu, S.; Zhang, Y. H. *Inorg. Chem.* **2007**, *46*, 795–800.
- (24) Delgado, S.; Gallego, A.; Castillo, O.; Zamora, F. *Dalton Trans.* **2011**, *40*, 847–852.
- (25) Raper, E. S. *Coord. Chem. Rev.* **1985**, *61*, 115–184.
- (26) Lobana, T. S.; Sharma, R.; Sharma, R.; Mehra, S.; Castineiras, A.; Turner, P. *Inorg. Chem.* **2005**, *44*, 1914–1921.
- (27) Yao, Y. G.; Cheng, J. K.; Chen, Y. B.; Wu, L.; Zhang, J.; Wen, Y. H.; Li, Z. J. *Inorg. Chem.* **2005**, *44*, 3386–3388.

- (28) Yao, Y. G.; Cheng, J. K.; Zhang, J.; Li, Z. J.; Cai, Z. W.; Zhang, X. Y.; Chen, Z. N.; Chen, Y. B.; Kang, Y.; Qin, Y. Y.; Wen, Y. H. *J. Chem. Am. Soc.* **2004**, *126*, 7796–7797.
- (29) Li, D.; Shi, W. J.; Hou, L. *Inorg. Chem.* **2005**, *44*, 3907–3913.
- (30) Givaja, G.; Amo-Ochoa, P.; Gómez-García, C. J.; Zamora, F. *Chem. Soc. Rev.* **2012**, *41*, 115–147.
- (31) Gou, S. H.; Zhu, H. B. *Coord. Chem. Rev.* **2011**, *255*, 318–338.
- (32) Alexandre, S. S.; Soler, J. M.; Miguel, P. J. S.; Nunes, R. W.; Yndurain, F.; Gomez-Herrero, J.; Zamora, F. *Appl. Phys. Lett.* **2007**, *90*, 193107.
- (33) Delgado, S.; Sanz Miguel, P. J.; Priego, J. L.; Jimenez-Aparicio, R.; Gomez-García, C. J.; Zamora, F. *Inorg. Chem.* **2009**, *47*, 9128–9130.
- (34) Armaroli, N.; Accorsi, G.; Cardinali, F.; Listorti, A. *Top. Curr. Chem.* **2007**, *280*, 69–115.
- (35) Delgado, S.; Barrilero, A.; Molina-Ontoria, A.; Medina, M. E.; Pastor, C. J.; Jimenez-Aparicio, R.; Priego, J. L. *Eur. J. Inorg. Chem.* **2006**, 2746–2759.
- (36) Delgado, S.; Medina, M. E.; Pastor, C. J.; Jimenez-Aparicio, R.; Priego, J. L. *Z. Anorg. Allg. Chem.* **2007**, *633*, 1860–1868.
- (37) Delgado, S.; Molina-Ontoria, A.; Medina, M. E.; Pastor, C. J.; Jimenez-Aparicio, R.; Priego, J. L. *Inorg. Chem. Commun.* **2006**, *9*, 1289–1292.
- (38) Leino, R.; Lonnqvist, J. E. *Tetrahedron Lett.* **2004**, *45*, 8489–8491.
- (39) Sheldrick, G. M. *SHELXS97 and SHELXL97*; University of Göttingen: Germany, 1997.
- (40) Farrugia, L. J. *J. Appl. Crystallogr.* **1999**, *32*, 837–838.
- (41) Hong, M. C.; Han, L.; Wang, R. H.; Wu, B. L.; Xu, Y.; Lou, B. Y.; Lin, Z. Z. *Chem. Commun.* **2004**, 2578–2579.
- (42) Zhang, X. M.; Hao, Z. M.; Wang, J. *Cryst. Eng. Commun.* **2010**, *12*, 1103–1109.
- (43) Zhang, X. M.; Hao, Z. M.; Fang, R. Q.; Wu, H. S. *Inorg. Chem.* **2008**, *47*, 8197–8203.
- (44) Addison, A. W.; Rao, T. N.; Reedijk, J.; Vanrijn, J.; Verschoor, G. C. *J. Chem. Soc., Dalton Trans.* **1984**, 1349–1356.
- (45) Bu, X. H.; Du, M.; Shang, Z. L.; Zhang, L.; Zhao, Q. H.; Zhang, R. H.; Shionoya, M. *Eur. J. Inorg. Chem.* **2001**, 1551–1558.
- (46) Journaux, Y.; Tuna, F.; Patron, L.; Andruh, M.; Plass, W.; Trombe, J. C. *J. Chem. Soc., Dalton Trans.* **1999**, 539–545.
- (47) Lee, S. C.; Holm, R. H. *Inorg. Chem.* **1993**, *32*, 4745–4753.
- (48) Yam, V. W. W.; Lo, K. K. W. *Chem. Soc. Rev.* **1999**, *28*, 323–334.
- (49) Turro, N. J. *Modern Molecular Photochemistry*; University ScienceBooks: Mill Valley, CA, 1991.
- (50) Ford, P. C.; Cariati, E.; Bourassa, J. *Chem. Rev.* **1999**, *99*, 3625–3647.
- (51) Vitale, M.; Rye, C. K.; Palke, W. E.; Ford, P. C. *Inorg. Chem.* **1994**, *33*, 561–566.
- (52) Redel, E.; Rohr, C.; Janiak, C. *Chem. Commun.* **2009**, 2103–2105.
- (53) Jagner, S.; Helgesson, G. *Adv. Inorg. Chem.* **1991**, *37*, 1–45.
- (54) Janiak, C.; Uehlin, L.; Wu, H. P.; Klufers, P.; Piotrowski, H.; Scharmann, T. G. *J. Chem. Soc., Dalton Trans.* **1999**, 3121–3131.
- (55) Arnbj, C. H.; Jagner, S.; Dance, I. *Cryst. Eng. Commun.* **2004**, *6*, 257–275.
- (56) Peng, R.; Li, M.; Li, D. *Coord. Chem. Rev.* **2010**, *254*, 1–18.
- (57) Habib, H. A.; Hoffmann, A.; Hoppe, H. A.; Steinfeld, G.; Janiak, C. *Inorg. Chem.* **2009**, *48*, 2166–2180.
- (58) Yam, V. W. W.; Wong, K. M. C. *Chem. Commun.* **2011**, *47*, 11579–11592.
- (59) Yam, V. W. W.; Lo, K. K. W. *Chem. Soc. Rev.* **1999**, *28*, 323–334.
- (60) Turro, N. J. *Modern Molecular Photochemistry*; University ScienceBooks: Mill Valley, CA, 1991.
- (61) Ford, P. C.; Cariati, E.; Bourassa, J. *Chem. Rev.* **1999**, *99*, 3625–3647.
- (62) Vitale, M.; Rye, C. K.; Palke, W. E.; Ford, P. C. *Inorg. Chem.* **1994**, *33*, 561–566.
- (63) Vogler, A.; Kunkely, H. *J. Am. Chem. Soc.* **1986**, *108*, 7211–7212.
- (64) Kyle, K. R.; Ryu, C. K.; Dibenedetto, J. A.; Ford, P. C. *J. Am. Chem. Soc.* **1991**, *113*, 2954–2965.
- (65) Galli, S.; Cariati, E.; Roberto, D.; Ugo, R.; Ford, P. C.; Sironi, A. *Inorg. Chem.* **2005**, *44*, 4077–4085.
- (66) Dai, J.; Zhou, J.; Bian, G. Q.; Zhang, Y.; Zhu, Q. Y.; Lu, W. *Inorg. Chem.* **2006**, *45*, 8486–8488.
- (67) Janiak, C. *Dalton Trans.* **2003**, 2781–2804.
- (68) Jiang, F. L.; Yue, C. Y.; Yan, C. F.; Feng, R.; Wu, M. Y.; Chen, L.; Hong, M. C. *Inorg. Chem.* **2009**, *48*, 2873–2879.
- (69) Song, J. L.; Dong, Z. C.; Zeng, H. Y.; Zhou, W. B.; Naka, T.; Wei, Q.; Mao, J. G.; Guo, G. C.; Huang, J. S. *Inorg. Chem.* **2003**, *42*, 2136–2140.